Available online at www.sciencedirect.com

SciVerse ScienceDirect

Ceramics International 38 (2012) 1065–1070

CERAMICS INTERNATIONAL

www.elsevier.com/locate/ceramint

Enhanced luminescence of novel $Ca_3B_2O_6:Dy^{3+}$ phosphors by Li^+-codoping for LED applications

Xin-Yuan Sun [a,b,*], Jun-Cheng Zhang [c], Xin-Gen Liu [a], Liang-Wu Lin [d]

[a] Department of Physics, Jinggangshan University, Ji'an 343009, PR China

[b] Key Laboratory for Ultrafine Materials of the Ministry of Education, East China University of Science and Technology, Shanghai, 200237, PR China

[c] Functional Materials Research Laboratory, Tongji University, Shanghai 200092, PR China

[d] State Key Laboratory for Powder Metallurgy, Central South University, Changsha, Hunan 410083, PR China

Received 25 July 2011; received in revised form 14 August 2011; accepted 15 August 2011

Available online 24 August 2011

Abstract

The $Ca_{3-x}B_2O_6:xDy^{3+}$ ($0.0 \le x \le 0.105$) and $Ca_{2.95-y}Dy_{0.05}B_2O_6:yLi^+$ ($0 \le y \le 0.34$) phosphors were synthesized at 1100 °C in air by solid-state reaction route. The as-synthesized phosphors were characterized by X-ray powder diffraction (XRD), scanning electron microscope (SEM), photoluminescence excitation (PLE) and photoluminescence (PL) spectra. The PLE spectra show the excitation peaks from 300 to 400 nm is due to the 4f–4f transitions of Dy^{3+}. This mercury-free excitation is useful for solid state lighting and light-emitting diodes (LEDs). The emission of Dy^{3+} ions upon 350 nm excitation is observed at 480 nm (blue) due to the $^4F_{9/2} \rightarrow {}^6H_{15/2}$ transitions, 575 nm (yellow) due to $^4F_{9/2} \rightarrow {}^6H_{13/2}$ transitions and a weak 660 nm (red) due to $^4F_{9/2} \rightarrow {}^6H_{11/2}$ emissions, respectively. The optimal PL intensity of the $Ca_{3-x}B_2O_6:xDy^{3+}$ phosphors is found to be $x = 0.05$. Moreover, the PL results from $Ca_{2.95-y}Dy_{0.05}B_2O_6:yLi^+$ phosphors show that Dy^{3+} emissions can be enhanced with the increasing codopant Li^+ content till $y = 0.22$. By simulation of white light, the CIE of the investigated phosphors can be tuned by varying the content of Li^+ ions, and the optimal CIE value (0.300, 0.298) is realized when the content of Li^+ ions is $y = 0.22$. All the results imply that the $Ca_{2.95-y}Dy_{0.05}B_2O_6:yLi^+$ phosphors could be potentially used as white LEDs.

Keywords: Solid-state reaction; Li^+-codoping; Photoluminescence; White LEDs

1. Introduction

As a potential candidate for replacement of conventional incandescent and fluorescent lamps, white LEDs have received extensive attention in recent years due to the advantages of long lifetime, saving energy, high efficiency, reliability and its environmental-friendly characteristics [1–3]. The most popular method to achieve white LEDs is phosphors-converted LEDs that use phosphors to convert the radiation of a near-ultraviolet (n-UV) or blue LED chip into white light. Currently, although two-band white LEDs using yellow-emitting YAG:Ce phosphors pumped by blue chips are dominant products in the market and white light is easily achieved by this method [4], several disadvantages appear for the practical application, including low colour rendering index and blue-halo effect for the lack of sufficient red emission [5,6]. Moreover, the observed white light varies with both the applied voltage of blue chips and the thickness of YAG phosphors, which results in its poor colour reproduction. Therefore, the design of some novel phosphors pumped by n-UV chips (350–410 nm) is of significance for white LEDs [7–9].

The borate-based phosphors have been of interest for using as a plasma panel display [10], the detection of dose of various energetic radiations [11] and white LEDs [5,12] in view of their large band-gap, low cost, excellent physical and chemical stability. The crystal structure of $Ca_3B_2O_6$ was reported to crystallize in the trigonal/rhombohedral system with a space group of $R-3C$ and the lattice parameters are $a = 8.6377$ Å, $b = 8.6377$ Å and $c = 11.849$ Å by Vegas et al. [13]. Recently, the luminescence properties of rare-earth-doped $Ca_3B_2O_6$ phosphors [14,15] and single crystal [16–18] have attracted intensive attention for their application in lamps, optical communication and scintillation fields, respectively. On the other hand, the visible luminescence of Dy^{3+} ($4f^9$) ion mainly

* Corresponding author. Tel.: +86 796 8100488.
E-mail address: sxy5306@126.com (X.-Y. Sun).

0272-8842/$36.00
doi:10.1016/j.ceramint.2011.08.032

consists of two intense bands in the blue and yellow regions, which are associated with the $^4F_{9/2} \rightarrow {}^6H_{15/2}$ and $^4F_{9/2} \rightarrow {}^6H_{13/2}$ transitions, respectively. The latter one is a hypersensitive transition, which is strongly influenced by the environment [19]. Namely, at a suitable yellow to blue (Y/B) intensity ratio, Dy^{3+} ions will emit white light. Thus, luminescent materials doped/codoped with Dy^{3+} ions are usually chosen to generate white-light [19–22]. To the best of our knowledge, there is no study on the luminescent properties of Dy^{3+} in $Ca_3B_2O_6$ host lattice. Herein, in the present work, luminescent properties and simulation of white-light for both $Ca_{3-x}B_2O_6{:}xDy^{3+}$ and $Ca_{2.95-y}Dy_{0.05}B_2O_6{:}yLi^+$ phosphors were investigated in detail by XRD, SEM and PL spectra, and the enhanced luminescence of $Ca_{2.95}Dy_{0.05}B_2O_6$ by codopant Li^+ were also discussed.

2. Experimental

Powder samples with stoichiometric composition of $Ca_{3-x}B_2O_6{:}xDy^{3+}$ (x = 0.0, 0.105, 0.205, 0.305, 0.07, 0.075, 0.09 and 0.105) and $Ca_{2.95-y}Dy_{0.05}B_2O_6{:}yLi^+$ (y = 0.0, 0.04, 0.10, 0.16, 0.22, 0.28 and 0.34) phosphors were synthesized by high temperature solid-state route. Raw materials of $CaCO_3$, H_3BO_3, Li_2CO_3 (Shanghai Chemical Reagent, A.R. grade) and Dy_2O_3 (Shanghai Yuelong New Materials Co. Ltd., 99.99%) were mixed thoroughly in an agate mortar. The amount of H_3BO_3 was excess of 5% to compensate its evaporation losses during the synthesis process. The well-ground mixtures were prefired at 700 °C for 60 min and subsequently calcined at 1100 °C for 300 min in air, then cool down naturally to room temperature.

The phase purity of the as-synthesized phosphors was investigated by X-ray powder diffraction spectroscopy (XRD) with a X-ray Diffractometer (Brucker D8) with Cu-Kα radiation at 40 kV and 40 mA. The XRD patterns were collected in the range of $25^\circ \leq 2\theta \leq 80^\circ$. The particle size and surface micrograph were observed by a scanning electric microscopy (JEOL, JSM-5510). The PL and PLE spectra were recorded on a luminescence spectrometer (Perkin-Elmer LS55), equipped with a 450 W xenon lamp as the excitation source. All the measurements were carried out at room temperature.

3. Results and discussion

3.1. Crystal structure and XRD analysis

The crystal structure of $Ca_3B_2O_6$ in rhombohedral representation is shown in Fig. 1. The basic elements of the structure are columns of calcium polyhedrons, with the coordination number (CN) with respect to oxygen equals to eight. All oxygen atoms coordinating calcium atoms enter the composition of nearly planar BO_3^{3-} groups isolated in the structure. It is well known that an acceptable percentage difference in ion radii between the doped and substituted ions must not exceed 30% [23], which suggests that both Dy^{3+} (1.027 Å, CN = 8) and Li^+ (0.92 Å, CN = 8) ions may prefer to substitute eight-coordinated Ca^{2+} ions (1.12 Å, CN = 8) rather than B^{3+} (0.15 Å) in the studied $Ca_3B_2O_6$ host lattice. Therefore, the general formula of the investigated phosphors is described as $Ca_{3-x}B_2O_6{:}xDy^{3+}$ and $Ca_{2.95-y}Dy_{0.05}B_2O_6{:}yLi^+$, respectively, where y denotes the substitution ratio of Dy^{3+} and Li^+ for Ca^{2+} ions.

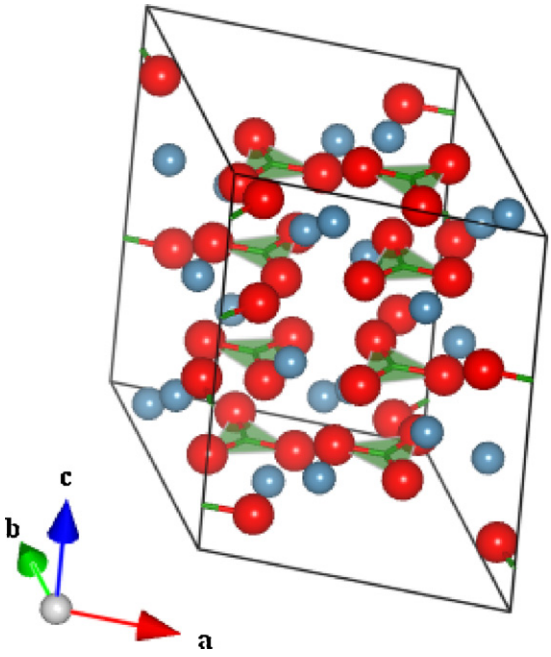

Fig. 1. Crystal structure of $Ca_3B_2O_6$.

The representative XRD patterns of the $Ca_{2.95-y}Dy_{0.05}B_2O_6{:}yLi^+$ phosphors with y = 0.0, 0.10, 0.22 and 0.34 are shown in Fig. 2. The diffractograms for all samples are similar and agree well with Joint Committee for Powder Diffraction Standard titled 26-0347 ($Ca_3B_2O_6$), indicating that samples are of single pure phase. The substitution of Ca^{2+} by both luminescence center (Dy^{3+}) and charge compensator (codopant Li^+) do not significantly influence the crystal structure, which clearly suggests that the dopant ions have been incorporated into the host lattice. Meanwhile, the full width at half maximum (FWHM) of the (1 1 3) peak near 30° is 0.178, 0.172, 0.164 and 0.174 for various Li^+ contents of 0.0, 0.12, 0.22 and 0.34, respectively. The decreased FWHMs in the XRD patterns with

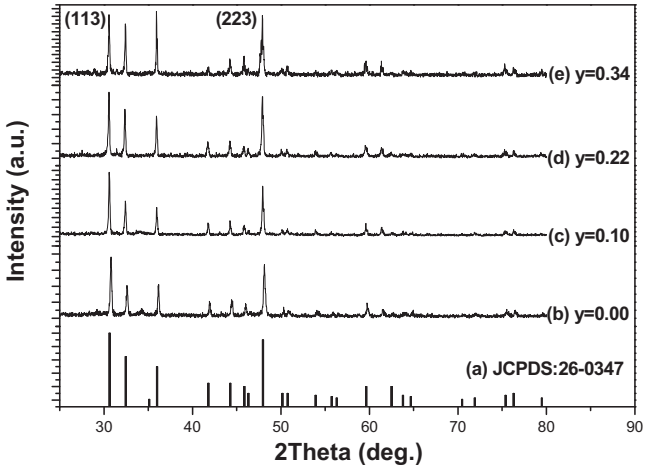

Fig. 2. XRD patterns of the standard data for $Ca_3B_2O_6$ and the representative $Ca_{2.95-y}Dy_{0.05}B_2O_6{:}yLi^+$ phosphors. (a) JCPDS 26-0347, (b) y = 0.00, (c) y = 0.10, (d) y = 0.22 and (e) y = 0.34.

the elevated Li^+ content till $y = 0.22$ show that the $y = 0.22$ sample has the best crystallinity. However, the FWHMs of the investigated phosphors increases when the Li^+ content exceeds 0.22 mol, implies that the crystallinity begin to get worse.

3.2. SEM analysis

The effect of codopant Li^+ ions on the surface morphology evolution for $Ca_{2.95-y}Dy_{0.05}B_2O_6:yLi^+$ phosphors is shown in Fig. 3. With respect to Fig. 3(a), whose grains agglomerate apparently, the grains in Fig. 3(b)–(d) get larger and more fine-shaped particles appear with the increase of Li^+ content till $y = 0.22$. The worse crystallinity of the $y = 0.34$ sample can be clearly observed, which are in line with the XRD pattern results. Both XRD and SEM results indicate that the crystallinity of the investigated phosphors can be controlled by adjusting the content of Li^+ ions, and the best crystallinity is found in the case of $y = 0.22$ samples.

3.3. Luminescence properties

3.3.1. $Ca_{3-x}B_2O_6:xDy^{3+}$

Fig. 4 shows the PLE and PL spectra of $Ca_{3-x}B_2O_6:xDy^{3+}$ ($x = 0.0$ and 0.05) phosphors, respectively. As shown in Fig. 4(b), the PL spectrum of Dy^{3+} ions consists of three emission regions: blue, yellow and weak red emission regions. The blue emission between 435 and 500 nm is assigned to the transition of Dy^{3+} ions from the $^4F_{9/2}$ to the $^6H_{15/2}$ ground state, while the yellow emission is observed in the wavelength region 555–595 nm, corresponding to the $^4F_{9/2} \rightarrow {}^6H_{13/2}$ optical transition of Dy^{3+}

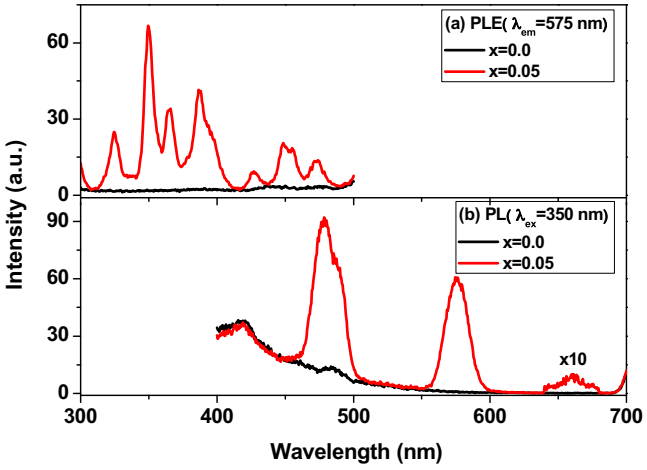

Fig. 4. PLE ($\lambda_{em} = 575$ nm) and PL ($\lambda_{ex} = 350$ nm) spectra of $Ca_{3-x}B_2O_6:xDy^{3+}$ phosphors (a) $x = 0.0$ and (b) $x = 0.05$.

ions. The red emission in vicinity of 661 nm (plotted by a factor of 10 in the wavelength 640–680 nm) is associated with the $^4F_{9/2} \rightarrow {}^6H_{11/2}$ optical transition. It is well known that the blue emission is of magnetic dipole origin and the yellow one is predominant only when Dy^{3+} are located at low-symmetry sites with no inversion centers [21]. Since emission intensity of the blue emission is stronger than that of the yellow one in the investigated phosphors, which suggests that there is very little deviation from inversion symmetry in the investigated phosphors. It is noteworthy there exists a broad emission centered at 416 nm in the blank phosphor ($x = 0.0$), and the emissions of Dy^{3+}-doped phosphor ($x = 0.05$) superposes the mentioned

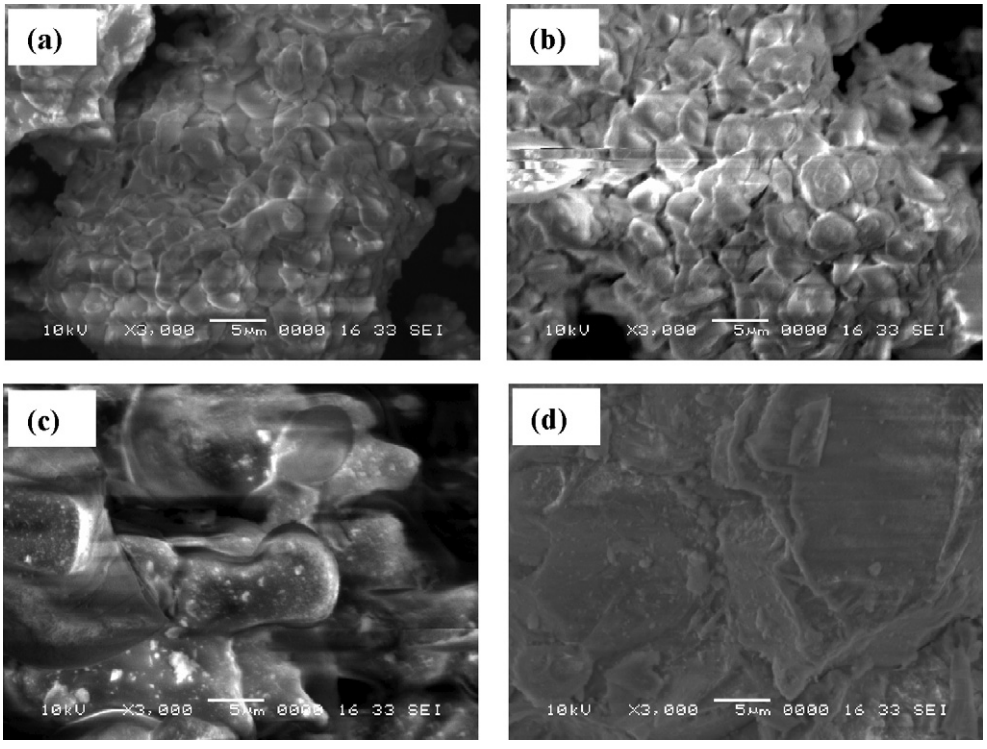

Fig. 3. SEM images of $Ca_{2.95-y}Dy_{0.05}B_2O_6:yLi^+$ phosphors (a) $y = 0.00$, (b) $y = 0.10$, (c) $y = 0.22$ and (d) $y = 0.34$.

broad emission. The results is very similar with that of $(Zn_{1-x}Tm_x)_2P_2O_7$ phosphors [24], but its origin needs further understanding.

As shown in Fig. 4(a), the excited bands centered at 324 nm ($^6H_{15/2} \rightarrow {}^4M_{17/2}$), 350 nm ($^6H_{15/2} \rightarrow {}^4M_{15/2}$, $^6P_{7/2}$), 366 nm ($^6H_{15/2} \rightarrow {}^4I_{11/2}$), 387 nm ($^6H_{15/2} \rightarrow {}^4I_{13/2}$, $^4F_{7/2}$), 427 nm ($^6H_{15/2} \rightarrow {}^4G_{11/2}$), 448 nm ($^6H_{15/2} \rightarrow {}^4I_{15/2}$) and 474 nm ($^6H_{15/2} \rightarrow {}^4F_{9/2}$) are observed when monitoring the 575 nm emission of Dy^{3+} ions. The profiles and position of these excitation peaks are not significantly influenced by various concentration of Li^+ ions due to the $4f^9$ electronic configuration of Dy^{3+} ions, and some strong excitation bands locating in the wavelength 350–410 nm imply that Dy^{3+} is of significance for n-UV white LEDs.

Fig. 5 shows the PL spectra of $Ca_{3-x}B_2O_6{:}xDy^{3+}$ phosphors excited by 350 nm light. The PL intensity of both blue and yellow emissions increases with the growing content of Dy^{3+} ions until reaching a maximum at $x = 0.05$, and then it decreases because of concentration quenching, as shown in the inset of Fig. 5.

The concentration quenching of the luminescence is due to the energy transfer from one activator to another until all the energy is consumed. For this reason, it is necessary to obtain the critical distance (R_c) that is the critical separation between donor (activators) and acceptors (quenching site). The critical distance R_c of the energy transfer between the same activators Dy^{3+} in $Ca_{3-x}B_2O_6{:}xDy^{3+}$ could be estimated according to the following equation [25]:

$$R_c = 2\left(\frac{3V}{4\pi x_c N}\right)^{1/3} \quad (1)$$

where x_c is the critical concentration, N is the number of Ca^{2+} ions in the unit cell and V is the volume of the unit cell. By taking the experimental and analytic values of x_c, N and V (0.05, 8 and 255.204 Å^3, respectively), the critical transfer distance of Dy^{3+} in $Ca_{3-x}B_2O_6{:}xDy^{3+}$ phosphors is estimated to be about 10.68 Å.

The energy levels of Dy^{3+} ions and visible emission are depicted in Fig. 6 according to the calculated data of energy levels by Carnall et al. [26]. When the 4f higher energy level of Dy^{3+} ions is excited by 350 nm n-UV light, the initial population relaxes to the lower energy levels until it arrives at the $^4F_{9/2}$ level by phonon-assisted process, then it give rise to the blue and yellow light as well as weak red emissions. With the elevated Dy^{3+} content, these characteristic emissions increase firstly before quenching concentration at $x = 0.05$, and subsequently decreases dramatically exceeds this critical concentration.

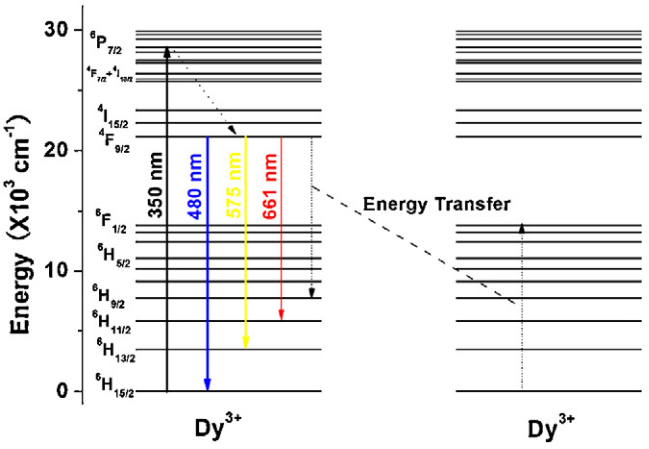

Fig. 6. Energy level diagrams, visible emission transition for Dy^{3+}, and the resonance energy transfer among Dy^{3+} ions.

3.3.2. $Ca_{2.95-y}Dy_{0.05}B_2O_6{:}yLi^+$

Fig. 7 displays the PL spectra of $Ca_{2.95-y}Dy_{0.05}B_2O_6{:}yLi^+$ phosphors. It is remarkable that both blue and yellow emission intensity of Dy^{3+} ions increase with the increasing content of Li^+ till $y = 0.22$, the emission intensity begin to decrease when the Li^+ content exceeds 0.22 mol. The strongest 575 nm emission intensity of the $y = 0.22$ phosphor is observed about six times higher than that of the sample without codopant Li^+. The enhanced luminescence of the studied phosphors, in our opinion, may be associated with both the flux effect and charge

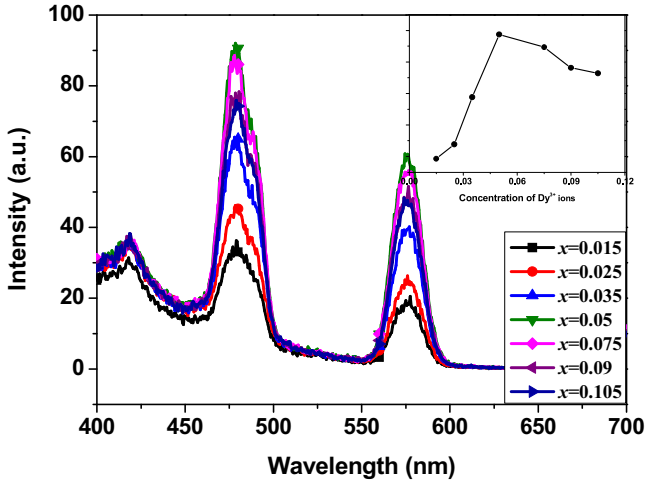

Fig. 5. PL spectra of $Ca_{3-x}B_2O_6{:}xDy^{3+}$ phosphors excited by 350 nm light. The inset shows the concentration dependence of Dy^{3+} 575 nm on codopant Li^+ ions.

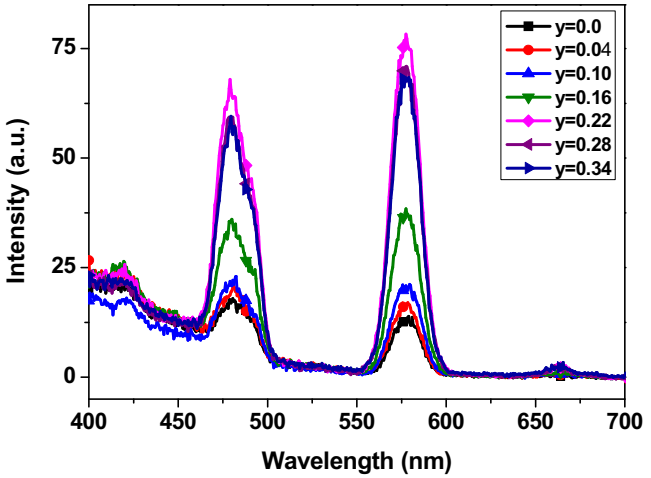

Fig. 7. PL spectra of the $Ca_{2.95-y}Dy_{0.05}B_2O_6{:}yLi^+$ phosphors excited by 350 nm light.

balance principle of Li^+ ions. On one hand, better crystallinity has been confirmed by XRD and SEM results (Figs. 2 and 3) with the growing Li^+ content till $y = 0.22$, leading to a lesser number of defects and stronger luminescence. The flux effect of the codopant Li^+ ions in luminescent phosphors has been testified elsewhere [27,28]. On the other hand, it is commonly accepted that some kinds of structure defects may form during the material synthesis at high-temperature. When Dy^{3+} is incorporated into $Ca_3B_2O_6$ host, it substitutes for a Ca^{2+} ion, which may induce structural defect $Dy_{Ca}^{\bullet}$. According to the principle of charge balance, the introduction of Dy^{3+} in $Ca_3B_2O_6$ should lead to the appearance of calcium ion vacancy, which can be expressed as the following equation:

$$2Dy_{Dy}^{x} + 3Ca^{x} \rightarrow 2Dy_{Ca}^{\bullet} + V_{Ca}'' \quad (2)$$

Generally, this negative vacancy is deleterious to the luminescence intensity of the Dy^{3+} ions because the energy transfer from the luminescence centers to the vacancy defects becomes more effective [29]. It is reasonable that in Fig. 7 the lowest intensity is observed for $Ca_{2.95}Dy_{0.05}B_2O_6$ ($y = 0.0$). The incorporation of Li^+ ions can neutralize the charge and prevent this vacancy formation. Charge balance is now attained via Eq. (3):

$$Dy_{Dy}^{x} + 2Ca_{Ca}^{x} + Li_{Li}^{x} \rightarrow Dy_{Ca}^{\bullet} + Li_{Ca}' \quad (3)$$

Thus, the introduction of Li^+ ions leads to the decrease of non-radiative transition probability and significantly increases the emission efficiency of Dy^{3+}-doped $Ca_3B_2O_6$ phosphors, as illustrated in Fig. 7.

It is well known that the blue emission is of magnetic dipole origin and the yellow one is electric dipole origin. The yellow ($^4F_{9/2} \rightarrow {}^6H_{13/2}$) emission is predominant only when Dy^{3+} ions are located at low-symmetry sites without inversion centers [21]. However, if the predominant emission is the blue one, it is an indication that the ligand-field deviates from inversion symmetry in the host. In order to learn the surrounding environments of Dy^{3+} ions, the peak intensity ratios of yellow to blue emission (Y/B) are calculated from their PL spectra and presented in Table 1. In contrast to the sample without codopant Li^+ ions, it is interesting that the yellow emission intensity begins to dominate

Table 1
Integral intensity ratios of yellow to blue emissions and chromaticity colour coordinations for $Ca_{2.95-y}Dy_{0.05}B_2O_6$:$yLi^+$ phosphors by 350 nm light excitation.

Colour coordination		$Ca_{2.95-y}Dy_{0.05}B_2O_6$:$yLi^+$		Y/B ratio	
		Peak intensity	Integral intensity	x	y
a	$y = 0.00$	0.758	0.556	0.259	0.232
b	$y = 0.04$	0.839	0.611	0.260	0.235
c	$y = 0.10$	0.990	0.749	0.291	0.276
d	$y = 0.16$	1.041	0.841	0.286	0.273
e	$y = 0.22$	1.188	0.990	0.300	0.298
f	$y = 0.28$	1.152	0.992	0.299	0.296
g	$y = 0.34$	1.212	1.000	0.299	0.295

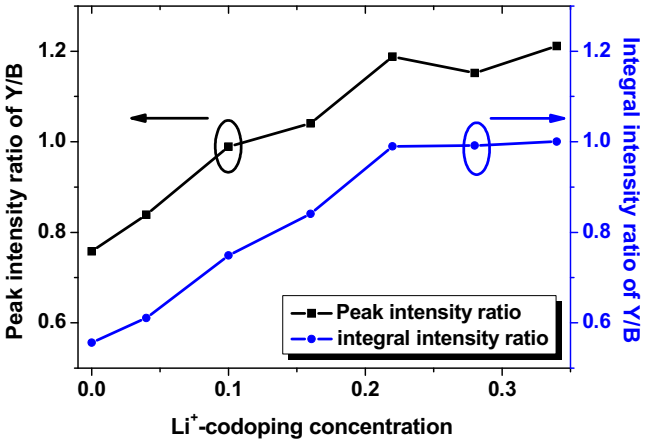

Fig. 8. Peak intensity ratio and integral intensity ratio of Y/B for $Ca_{2.95-y}Dy_{0.05}B_2O_6$:$yLi^+$ phosphors.

obviously over the blue one when the content of Li^+ ions exceeds 0.16 mol, and the peak intensity ratio of the yellow to blue (Y/B) increases with the increase of Li^+ content, as also shown in Fig. 8. With the increase of Li^+ content, the predominant emission from blue to yellow zone implies that the surrounding environment of Dy^{3+} ions may have been changed remarkably. However, as depicted in the crystal structure of the $Ca_3B_2O_6$, there exists only one calcium ions site with eight oxygens coordination. The possible mechanism of such a change is in progress.

3.4. Simulation of white light

For comparison with the peak intensity ratio of Y/B, the integral intensity ratios of Y/B in the $Ca_{2.95-y}Dy_{0.05}B_2O_6$:$yLi^+$ phosphors are presented in Table 1. It is found that the integral intensity ratios of Y/B increase with the additive Li^+ ions. The change in the Y/B ratio is attributable to the change of the environment around Dy^{3+} ions as it involves a hypersensitive transition $^4F_{9/2} \rightarrow {}^6H_{13/2}$ with $\Delta J = 2$. It is worth to note that the Y/B ratios change little after concentration quenching indicating that the environment of the Dy^{3+} ions may be less influenced due to the cluster of the Dy^{3+} ions after concentration quenching [30].

The variation of Y/B intensity ratios indicates the feasibility of the generation of white light in the investigated phosphors. The chromaticity colour coordinates for $Ca_{2.95-y}Dy_{0.05}B_2O_6$:$yLi^+$ phosphors are simulated and also listed in Table 1. The corresponding Commission International de I'Eclairage (CIE) 1931 x–y chromaticity diagram are presented in Fig. 9, and the inset simultaneously shows the enlarged spectrum for colour coordinate (x) value from 0.255 to 0.305. With the increase of Li^+ ions, the chromaticity colour coordinates can be tuned efficiently from the border of white region to its equal-energy white light point. The best value (0.300, 0.298) is achieved when $y = 0.22$, which implies that the investigated phosphors can be potentially used as white LEDs.

4. Conclusions

In summary, novel $Ca_{3-x}B_2O_6$:xDy^{3+} and $Ca_{2.95-y}Dy_{0.05}B_2O_6$:$yLi^+$ phosphors for white LEDs have been successfully

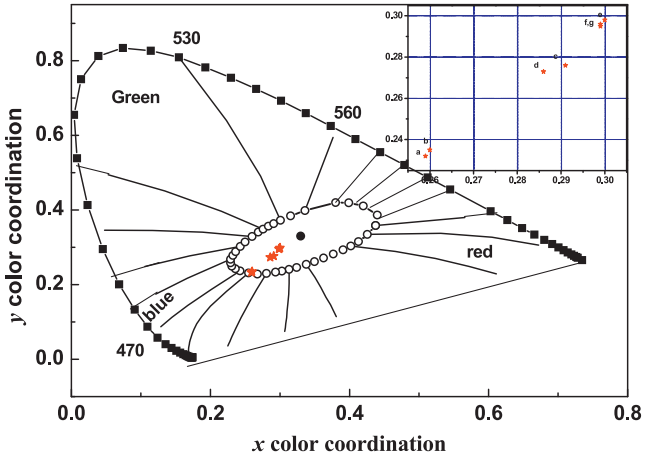

Fig. 9. CIE coordinate diagram of $Ca_{2.95-y}Dy_{0.05}B_2O_6$:$yLi^+$ phosphors by 350 nm light, the inset shows the enlarged spectrum for colour coordinate (x) value from 0.255 to 0.305.

synthesized and their luminescent properties been investigated. Better crystallinity and perfect microscopy can be controlled by codoping with proper Li^+ ions. The PL results of $Ca_{3-x}B_2O_6$:xDy^{3+} phosphors shows that the strongest luminescence is $x = 0.05$, and its emission intensity can be further enhanced about six times by codoping with 0.22 mol Li^+. The enhanced emission of Dy^{3+} ions in $Ca_3B_2O_6$ host is attributive to both the flux effect and charge compensation of Li^+ ions. The corresponding colour coordination can also be efficiently tuned by controlling Li^+ content, and the optimal CIE value (0.300, 0.298) is realized when $y = 0.22$. It is close to the equal-energy white light point (0.333, 0.333), which implies that the investigated phosphor can be potentially used as n-UV white LEDs.

Acknowledgements

We wish to acknowledge our gratitude to the financial support provided by the National Natural Science Fund of China (Grant No. 11165010), the Specialized Research Fund for the Doctoral Program of Higher Education (Grant No. 20090162120008), Open Fund of Key Laboratory for Ultrafine Materials of the Ministry of Education, East China University of Science and Technology, and the Program for Young Excellent Doctors in Jinggangshan University.

References

[1] A. Bergh, G. Craford, A. Duggal, R. Haitz, The promise and challenge of solid-state lighting, Phys. Today 54 (2001) 42–47.
[2] A.H. Narendran, M.A. Petruska, M. Achermann, D.J. Weeder, E.A. Akhadov, D.D. Koleske, M.A. Hoffbauer, V.I. Klimov, Multicolor light-emitting diodes based on semiconductor nanocrystals encapsulated in GaN charge injection layers, Nanoletters 5 (2005) 1039–1044.
[3] A. Kitai, Luminescenct Materials and Application, John Wiley & Sons, Ltd., 2008,, p. 75.
[4] S. Nakamura, G. Fasol, The Blue Laser Diode, Spring, Berlin, 1997, p. 87.
[5] C.K. Chang, T.M. Chen, $Sr_3B_2O_6$:Ce^{3+},Eu^{2+}: a potential single-phased white-emitting borate phosphor for ultraviolet light-emitting diodes, Appl. Phys. Lett. 91 (2007), 081902:1–3.
[6] C.C. Chiang, M.S. Tsai, M.H. Hon, Preparation of cerium-activated GAG phosphors powders influence of co-doping on crystallinity and luminescent properties, J. Electrochem. Soc. 154 (2007) J326–J329.
[7] J. Huang, L. Zhou, Q. Pang, F. Gong, J. Sun, W. Wang, Photoluminescence properties of a novel phosphor CaB_2O_4:Eu^{3+} under NUV excitation, Luminescence 24 (2009) 363–366.
[8] W.S. Song, Y.S. Kim, H. Yang, Yellow-emitting phosphor of $Sr_3B_2O_6$:Eu^{2+} for application to white light-emitting diodes, Mater. Chem. Phys. 117 (2009) 500–503.
[9] C. Qin, Y. Huang, L. Shi, G. Chen, X. Qiao, H.J. Seo, Thermal stability of luminescence of $NaCaPO_4$:Eu^{2+} phosphor for white-light-emitting diodes, J. Phys. D: Appl. Phys. 42 (2009), 185105:1–5.
[10] C. Kulshreshtha, S.H. Cho, Y.S. Jung, K.S. Sohn, Deep red color emission in an sm^{2+}-doped SrB_4O_7 phosphor, J. Electrochem. Soc. 154 (2007) J86–J90.
[11] L. Liu, Y. Zhang, J. Hao, C. Li, Q. Tang, C. Zhang, Q. Su, Thermoluminescence characteristics of terbium-doped $Ba_2Ca(BO_3)_2$ phosphor, Phys. Status Solidi A 202 (2005) 2800–2806.
[12] H. Lin, H. Liang, B. Han, J. Zhong, Q. Su, Luminescence and site occupancy of Ce^{3+} in $Ba_2Ca(BO_3)_2$, Phys. Rev. B 76 (2007) 035117.
[13] A. Vegas, F.H. Cano, S.G. Blanco, The crystal structure of calcium orthoborate: a redetermination, Acta Crystallogr. B 31 (1975) 1416–1419.
[14] D. Voort, J.M.E. Rijk, R. Doorn, G. Blasse, Luminescence of rare-earth ions in $Ca_3(BO_3)_2$, Mater. Chem. Phys. 31 (1992) 333–339.
[15] I.V. Berezovskaya, N.P. Efryushina, P.A. Rodnyi, A.S. Voloshinovskii, V.P. Dotsenko, Luminescence of calcium orthoborate doped by Ce^{3+} ions, Opt. Spectrosc. 101 (2006) 902–905.
[16] X. Liu, Z. You, J. Li, Z. Zhu, G. Jia, Y. Wang, B. Wu, C. Tu, Growth and properties of pure and rare earth-doped $Ca_3(BO_3)_2$ single crystal, J. Cryst. Growth 281 (2005) 416–425.
[17] X. Liu, Z. You, J. Li, Z. Zhu, G. Jia, B. Wu, C. Tu, Optical properties of Er^{3+} doped $Ca_3(BO_3)_2$ crystal, J. Appl. Phys. 100 (2006), 033103:1–5.
[18] Q. Su, Z. Pei, L. Chi, H. Zhang, Z. Zhang, D. Zhou, The yellow-to-blue intensity ratio (Y/B) of Dy^{3+} emission, J. Alloys Compd. 192 (1993) 25–27.
[19] Y. Fujimoto, T. Yanagida, Y. Yokota, N. Kawaguchi, K. Fukuda, D. Totsuka, K. Watanabe, A. Yamazaki, A. Yoshikawa, Scintillation characteristics of Tm^{3+} in $Ca_3(BO_3)_2$ crystals, Radiat. Meas. (2011), doi:10.1016/j.radmeas.2011.03.038.
[20] A. Diza, D.A. Keszler, Eu^{2+} Luminescence in the Borates $X_2Z(BO_3)_2$ (X = Ba, Sr; Z = Mg, Ca), Chem. Mater. 9 (1997) 2071–2077.
[21] B. Liu, C. Shi, Z. Qi, Potential white-light long-lasting phosphor:Dy^{3+}-doped aluminate, Appl. Phys. Lett. 86 (2005), 191111:1–3.
[22] B.V. Ratnam, M. Jayasimhadri, K. Jang, H.S. Lee, S.S. Yi, J.H. Jeong, White light emission from $NaCaPO_4$:Dy^{3+} phosphor for ultraviolet-based white light-emitting diodes, J. Am. Ceram. Soc. 93 (2010) 3857–3861.
[23] B. Liu, Y. Wang, J. Zhou, F. Zhang, Z. Wang, The reduction of Eu^{3+} to Eu^{2+} in $BaMgAl_{10}O_{17}$:Eu and the photoluminescence properties of $BaMgAl_{10}O_{17}$:Eu^{2+} phosphor, J. Appl. Phys. 106 (2009), 053102:1–5.
[24] M. Peng, Z. Pei, G. Hong, Q. Su, The reduction of Eu^{3+} to Eu^{2+} in $BaMgSiO_4$:Eu prepared in air and the luminescence of $BaMgSiO_4$:Eu^{2+} phosphor, J. Mater. Chem. 13 (2003) 1202–1205.
[25] G. Blasse, Energy transfer in oxides phosphors, Philips Res. Rep. 24 (1969) 131–136.
[26] W.T. Carnall, P.R. Fields, K. Rajnak, Electronic energy levels in the trivalent lanthanide aquo ions. I. Pr^{3+}, Nd^{3+}, Pm^{3+}, Sm^{3+}, Dy^{3+}, Ho^{3+}, Er^{3+}, and Tm^{3+}, J. Chem. Phys. 49 (1968) 4424–4442.
[27] X. Liu, K. Han, M. Gu, L. Xiao, C. Ni, S. Huang, B. Liu, Effect of codopants on enhanced luminescence of $GdTaO_4$:Eu^{3+} phosphors, Solid State Commun. 142 (2007) 680–684.
[28] F.C. Park, H.K. Moon, D.K. Kim, S.H. Byeon, B.C. Kim, K.S. Suh, Morphology and cathodoluminescence of Li-doped Gd_2O_3:Eu^{3+}, a red phosphor operating at low voltages, Appl. Phys. Lett. 77 (2000) 2162–2164.
[29] V.P. Dotsenko, I.V. Berezovskaya, N.P. Efryushina, A.S. Voloshinovskii, P. Dorenbos, C.W.E. van Eijk, Luminescence of Ce^{3+} ions in strontium haloborates, J. Lumin. 93 (2001) 137–145.
[30] X. Sun, S. Huang, X. Gong, Q. Gao, Z. Ye, C. Cao, Spectroscopic properties and simulation of white-light in Dy^{3+}-doped silicate glass, J. Non-cryst. Solids 356 (2010) 98–101.